

Please fill in the name of the event you are preparing this manuscript for.	SPE Annual Technical Conference and Exhibition 2020
Please fill in your 6-digit SPE manuscript number.	SPE-201285-MS
Please fill in your manuscript title.	A New Computational Fluid Dynamics Model To Optimize Sucker Rod Pump Operation And Design

Please fill in your author name(s) and company affiliation.

Given Name	Surname	Company
Shreyas V.	Jalikap	AC2T research GmbH
Bernhard	Scheichl	AC2T research GmbH; Technische Universität Wien, Institute of Fluid Mechanics and Heat Transfer
Stefan J.	Eder	AC2T research GmbH; TU Wien, Institute of Engineering Design and Product Development
Stefan	Hönig	OMV Exploration & Production GmbH, TECH Center & Lab

This template is provided to give authors a basic shell for preparing your manuscript for submittal to an SPE meeting or event. Styles have been included (Head1, Head2, Para, FigCaption, etc) to give you an idea of how your finalized paper will look before it is published by SPE. All manuscripts submitted to SPE will be extracted from this template and tagged into an XML format; SPE's standardized styles and fonts will be used when laying out the final manuscript. Links will be added to your manuscript for references, tables, and equations. Figures and tables should be placed directly after the first paragraph they are mentioned in. The technical content of your paper WILL NOT be changed. Please start your manuscript below.

Abstract

Artificial lift systems are widely used in oil production, of which sucker rod pumps are conceptually among the simpler ones. The reciprocating movement of the plunger triggers the opening and closing of two ball valves, allowing fluid to be pumped to the surface. Their built-in ball valves are subject to long-time erosion and fail as a consequence of this damage mechanism. Understanding the principal damage mechanisms requires a thorough examination of the fluid dynamics during the opening and closing action of these valves.

In this paper we present a fluid–structure interaction model that simultaneously computes the fluid flow in the traveling valve, the standing valve, and the chamber of sucker rod pumps during a full pump cycle. The simulations shed light on the causes of valve damage for standard and non-ideal operating conditions of the pump. In particular, our simulations based on real pump operating envelopes reveal that the so-called “mid-cycle valve closure” is likely to occur. Such additional closing and opening events of the valves multiply situations where the flow conditions are harmful to the individual pump components, leading to efficiency reduction and pump failure. This mechanism, hitherto unappreciated in the literature, is believed to constitute the primary cause of long-term valve damage.

Our finite element method (FEM) based computational-fluid-dynamics model can accurately describe the opening and closing cycles of the two valves. For the first time, this approach allows an analysis of real traveling valve speed versus position plots, usually called pump cards. The effects of stroke length, plunger speed and fluid parameters, on the velocity and pressure at any point and time inside the pump can thus be investigated. The Identifying damage-critical flow parameters can help suggest measures to avoid unfavorable operating envelopes in future pump designs.

Our flow model may support field operations throughout the entire well life, ranging from improved down-hole pump design to optimized pump operation or material selections. It can aid the creation of an ideal interaction between the valves, thus avoiding “mid-cycle valve closure” to drastically extend the mean time between failures of sucker rod pumps. Finally, our simulation

approach will speed up new pump component development while greatly reducing the necessity for costly laboratory testing.

Introduction

Sucker rod pumps for artificial lift are one of most widely used methods of oil production. The operating principle of the major parts of a sucker rod pump is that fluid is hoisted to the surface by reciprocating plunger operation. The pumped fluid volume per pump stroke is regulated by the alternating opening and closing actions of two ball valves, called the traveling valve (TV) and standing valve (SV). The only essential moving parts here are the plunger and the check balls within the cages of the valves. Yet, the oil industry constantly faces problems with material damage to the valves, such as ball-seat impact damage leading to erosion in the long term that contribute to more than half of the failures in sucker rod pump based artificial lift assemblies (Hoy et al. 2018). Although fluid dynamics related phenomena such as fluid pound, gas formation etc. are known to cause pump damage (Samad 2010, Lyons et al. 2016), their source is usually complex and not well understood. This is because the pumps operate hundreds of meters below the surface, and monitoring the operation of the valve is impracticable. In particular, the information about the opening and closing states of the two ball valves, the TV and the SV in realistic operating conditions, is not known. For example, Cutler and Mansure (1999) discuss partially open valves as a possible cause of ball chatter, but cannot confirm this from their model. Hence, modeling and simulations are important in understanding how sucker rod pumps behave under realistic operating conditions, which in turn helps us understand the damage mechanisms discussed above.

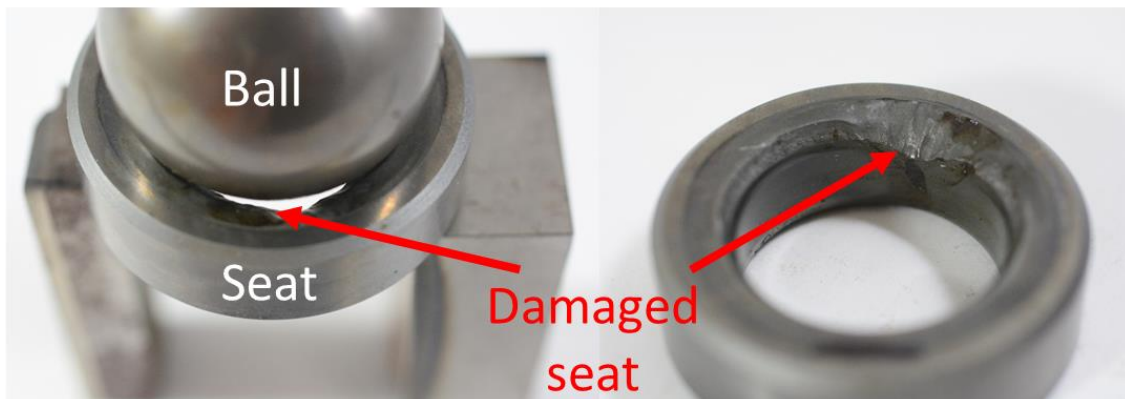


Figure 1 Images of ball and seat of a traveling valve showing severe damage that may occur during operation in a down-hole pump. The pictured ball and seat come from a 225-dimension pump and consist of TiC-WC and WC with densities of 9.1 and 13.9 g/cm³, respectively. The valve was removed from a depth of 1200 m of a vertical well after 1034 days of operation and 8.2 million strokes (stroke length 2.04 m, 5.5 strokes/min). Only small amounts of sand were found in the pump, and the discharge pressure was 125 bar.

The current work was the result of an evolving study focused on addressing the above mentioned problem with the goal to identify and individuate critical operating conditions and design of pump components. It was observed that the damage on the valve seat mostly occurred in the region where the ball-seat contact occurred, see Figure 1. Hence, the effect of impact on commercially available pump valve materials was considered. Various tests to investigate their resistance to mechanical impact force and its consequences to the material structure when the ball hits the valve seat were executed to improve the understanding of critical parameters that cause pump failures (Katsich *et al.*, 2019). During these tests, a closer look at the exact region of damage revealed that in some cases, the actual damage occurred some distance away from

the line of ball-seat contact, where mechanical impact could not have directly caused the damage. Hence, the role of fluid dynamics related phenomena was suspected, and a mathematical model that describes the fluid flow inside a sucker rod pump and allows the easy determination of critical flow and operating parameters for sucker rod pumps was developed. An additional project demand was that the mathematical model be able to simulate realistic pump cycles, calculating fluid flow at both valves and inside the pump barrel. This facilitates the study of fluid flow conditions at each instant of the pumping sequence as well as an understanding or prediction of its potential damaging influence to any component of a sucker rod pump.

A comprehensive literature research revealed a rich variety of different flow models and their implementations into finite-element schemes for calculating the sucker rod pump behavior in forerunner studies. They consider fluid effects on the valves through lumped fluid forces (Doty and Schmidt, 1983; Lekia & Evans, 1995, Lannetti *et al.*, 2014; Domnick *et al.*, 2017; Domnick & Brillert, 2019), but do not take the detailed fluid flow into consideration to reproduce the coupled movements of the valves. Although flow-related damage mechanisms of down-hole pumps are described, the actual causes of material degradation are neither clearly explained nor fully understood. Our computations predict sudden pressure drops in valves that might lead to release of dissolved gases. Gas accumulation, which is associated with non-ideal operating conditions, is known to cause pump damage (Lyons *et al.*, 2016). These pressure drops are, however, distinct from those that cause cavitation damage in valves operating on the surface. This is because, the absolute hydrostatic pressure in a down hole pump is usually large enough to prevent any local vaporization of pumped fluid. Hence, we do not consider cavitation phenomenon in our model.

The first computational fluid dynamics simulations were developed and refined for accurately estimating loads on the tubing and sucker rods caused by fluid-structure interaction (Cutler & Mansure, 1999, Romero & Almeida, 2014). Our newly developed computational fluid dynamics model focuses on mathematically describing the fluid flow and material resistance under realistic operating conditions. It is applied to investigate the influence that pump hardware and pump operating parameters such as, but not limited to, pump cage dimensions, stroke length, plunger speed, ball densities, seat materials, or ball impact forces have on the overall performance and expected resistance of the valve seats and balls to fluid flow. The simulator predicts the expected operating movements of the ball valves, the resulting fluid flow velocities, and it can identify critical flow conditions that may cause material wear. By focusing on the precise working of the coupled valves, the model contributes a crucial knowledge towards a growing number of models aimed at improving prediction of the working of the sucker rod pump in realistic conditions. For example, Li *et al.* (2018) highlight the importance of considering the movement of fluid flowing into the pump with the instantaneous dissolution and evolution of gas. This is included in their comprehensive model of the entire sucker rod pump, however, the critical conditions which determine a particular flow state can be provided by our model.

Our simulations of the actual pump cycle behavior of sucker rod pumps point to a non-ideal operating scenario associated with the mutual interaction between the valves, referred to as “mid-cycle valve closure” henceforth. By setting the time-variable plunger speed to values obtained from actual pump dynamometer cards, the fluid flow and resulting forces on the two balls of the ball valves were calculated for a full periodic pump cycle; particular emphasis was placed on the movements of the balls. The calculations show that in non-ideal operating modes the ball valve is indeed prone to closing one or several times during a pumping cycle. This additional closing and re-opening of the ball valve increases fluid dynamical flow conditions that are critical to the pump component materials and may therefore reduce the lifetime of the pump. The developed model allows us to investigate and predict these critical operating situations. Modifying the operating or geometric design parameters will help engineers with selecting the best pump design and operating modes so as to reduce the risk or even eliminate the

phenomenon of mid-cycle valve closure, thus increasing the lifetime of the entire pump. Novel pump or pump component developments such as innovative plunger, standing and traveling valve as well as cage designs, or the educated selection of the ball material and hence its density, will benefit from these simulations and the understanding of critical flow parameters in sucker rod pumps.

In the following section we briefly describe the model and the assumptions made in the model and its capabilities. In section 3, we describe the valve closing and opening process to show how pump parameters affect the valve operation. In chapter 4, we apply the model to analyze a pump card (plunger speed versus position plot) from a real pump to show how certain operating conditions or pump design can lead to pressure drops that are dangerous for that pump. In the last section, we summarize the results.

Model description

We first discuss the assumptions the computational model is based on and justify its bounds of applicability. These assumptions are justified by validating the model with existing literature on force measurements on the ball of check valves. The reader is referred to Jalikop *et al.* (2019) for the details of the validation procedure and the model in general. The computations were carried out in a finite element (FE) based software, COMSOL Multiphysics 5.2a. A run of the simulation for two pump cycles took up to a day on AMD Ryzen 9 16-Core CPU desktop. The computations were verified for mesh convergence, the details of which are provided in the above publication along with the details of the meshing procedure.

Basic ingredients

Our model abstracts the down-hole pump by focusing on the dynamic coupling between the two ball check valves, the SV and the TV. The computational domain of the model comprises of the two valves and the chamber in-between the valves, where the volume is expanding and contracting as the plunger moves up and down (see Figure 2 (a)). Any predefined kinematics of the TV can be imposed as an input, and so can the hydrodynamic pressure at the inlet and the outlet of the domain, representing the pump intake pressure (PIP) and the tubing pressure (TP), respectively. The balls in the valve cages are free to move up and down over a distance l (see Figure 2 (b)) within the valve cage. Their motion is governed by the net force resulting from the balance between the weight of the ball and the hydrodynamic forces exerted on them by the fluid being pumped. The elastic deformations of the pump materials are assumed to be negligible, and the fluid is considered to be of a single phase with uniform physical properties and Newtonian. The flow is laminar and incompressible. For the details of our pump model and its validation against existing literature the reader is referred to Jalikop *et al.* (2019). However, we discuss some of the salient features of the model in the following few paragraphs.

The full Navier–Stokes equations are solved using a finite-element discretization that employs a moving-mesh approach to accommodate the temporal variation of the size of the chamber. The flow is assumed to be axisymmetric, laminar, and incompressible. The motion of the ball within the valve cage is severely restricted in the transverse direction by the wall of the valve cage. The presence of a wall has two main effects: the first is that it reduces the instability of the flow behind the ball and secondly it induces transverse forces on the ball that center the ball along the axis. Hence, the assumption of the axisymmetric flow does not severely limit the validity of the model. We treat the flow as laminar, the main reason being that the computational burden of employing a turbulent model outweighs the gain in accuracy of estimation of the drag force on the ball, especially when we are interested in the dynamics on the scale of plunger

kinematics. Because the main aim of the work is to demonstrate the nature of the interaction between the coupled valves, we chose the computational feasibility of simulating the entire pump cycle in a single model over numerical accuracy. Moreover, choosing the right turbulent model for a complex system such as the down-hole pump can introduce its own uncertainties.

Modeling the process of valve closing is particularly challenging, as this process terminates in the rupture of the fluid film when the gap formed by the ball and the seat closes to give way to inevitable solid-solid contact. This results in the break-down of the continuum hypothesis on which the finite element method is based on, and hence requires a special numerical treatment over a small time scale. A similar difficulty is encountered during the valve opening process because of the fluid entrainment into the gap forming just after the ball has lost contact with the seat. The novel technique to overcome these problems employs a repulsive force exerted on the ball as it approaches/departs from the seat such that a very thin layer of fluid between the ball and the seat is always present, fictitiously even in the fully closed position of the valve. Accepting a thereby “slightly leaking”, as incompletely closing, valve outweighs by far any much more sophisticated alternative in dealing with the discontinuities formed in the fluid violating the continuum hypothesis as intrinsic to the real physical process. Moreover, the thickness of the remaining fluid layer can be made arbitrarily small in principle, where the limitation is found by due considerations regarding computational stability and feasibility. Although the repulsive force is an empirical construct used to aid our simulations, it is not an entirely unphysical force. Such forces, which prevent solid–solid contact, are predicted by the locally valid lubrication approximation of the governing equations in the limit of an infinitely thin gap (Davis *et al.*, 1986; Scheichl *et al.*, 2015).

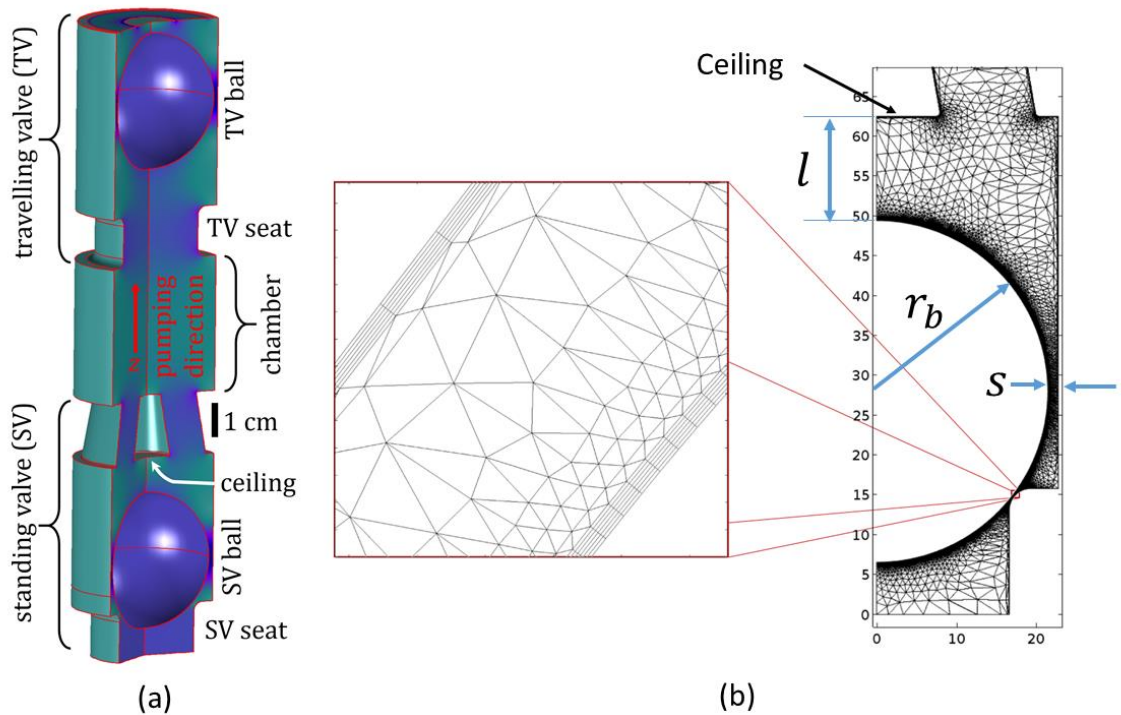


Figure 2 (a) Schematic of the pump consisting of two ball check valves and the expanding and contracting chamber in between. (b) Typical mesh for axisymmetric FEM simulations in half-space, along with the important geometrical parameters of the valve. For the simulation results presented here, we have considered $r_b = 0.02144$ m, $s = 0.00135$ m and $l = 0.0467$ m and 0.0592 m for SV and TV, respectively. The standard numbers for the ball and the seat are V12-250 and V13-250, respectively.

Capabilities of the model

Using the model, one can simulate the complete laminar flow field within the valves and the chamber, including the motion of the check balls in the cage of the valve (see Figure 2). Using this flow field data and working within the assumptions that are described above, the model is capable of providing us the following information of a down-hole pump.

- Dynamic interaction of the two ball check valves through fluid dynamic forces
- Opening/closing states of the two valves
- Ball speeds as a function of time and position
- Fluid pressure; especially in the gap between the ball and the seat, where the pressure drop information is crucial in understanding the damage mechanism
- Real pump-card data can be used as input for the plunger kinematics, including the full stroke lengths of the pumping action
- Parametric studies of pumping by varying the geometry, plunger kinematics or the material properties of the ball and fluid medium

Valve operation

It is important to understand the effect of dynamic coupling between the TV and SV on the pump operation to be able to optimize the pump design parameters. In this section, we employ our model to study the effect of some of the pump parameters on the pump operation from a fluid dynamics perspective. We simulate the dynamics of the ball during the opening/closing of the SV to compute the approach speed of the ball during the closing process and the fluid dynamic forces needed to lift the ball off the seat during opening process. In particular, we study the influence of the density of the ball material (or the ball weight) and the speed of the plunger. Accurate estimates of the ball speeds during approach towards the seat is also important to avoid undesirable ball-seat impacts.

The geometry of the pump used in all our simulations is shown in Figure 2(b), and the values of the parameters considered were; $\rho_b = 9 \text{ g/cm}^3$, $\rho_f = 1 \text{ g/cm}^3$, $\nu = 1 \text{ cS}$, and the pressure non-dimensionalized by (PIP-TP) = 0.5 bar. We have chosen a small value for (PIP-TP) compared to the values typically seen in the field. This is to aid computations so that the repulsive force employed in the valve closing process does not become unnecessarily too large, which might otherwise lead to computational instabilities. Moreover, we expect this pressure difference to have any influence at all on the motion of the balls only in the extremely rare scenario when both the valves are open at the same time, which we do not encounter in our simulations.

Valve closing

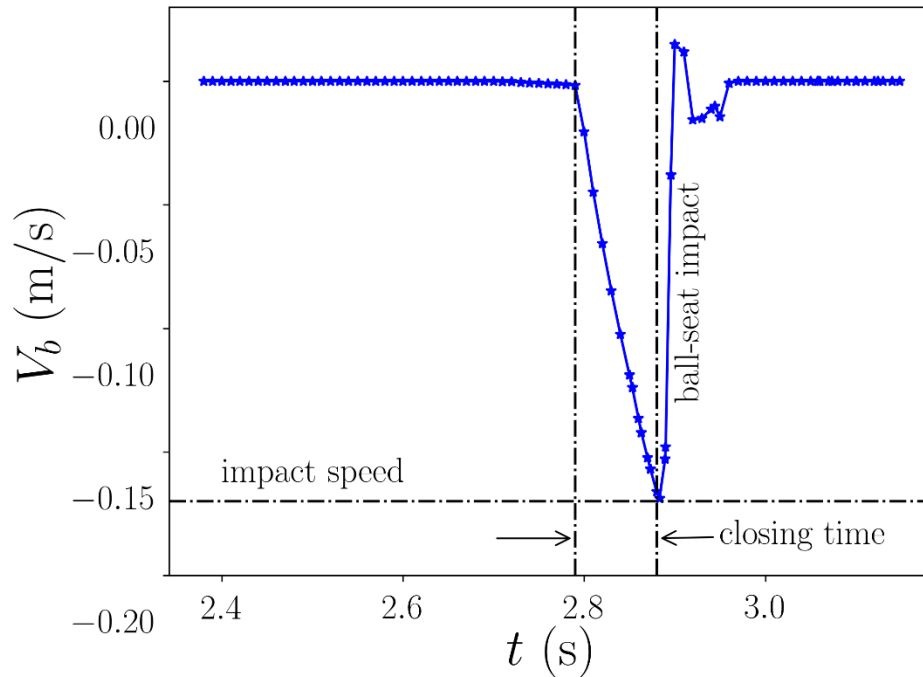
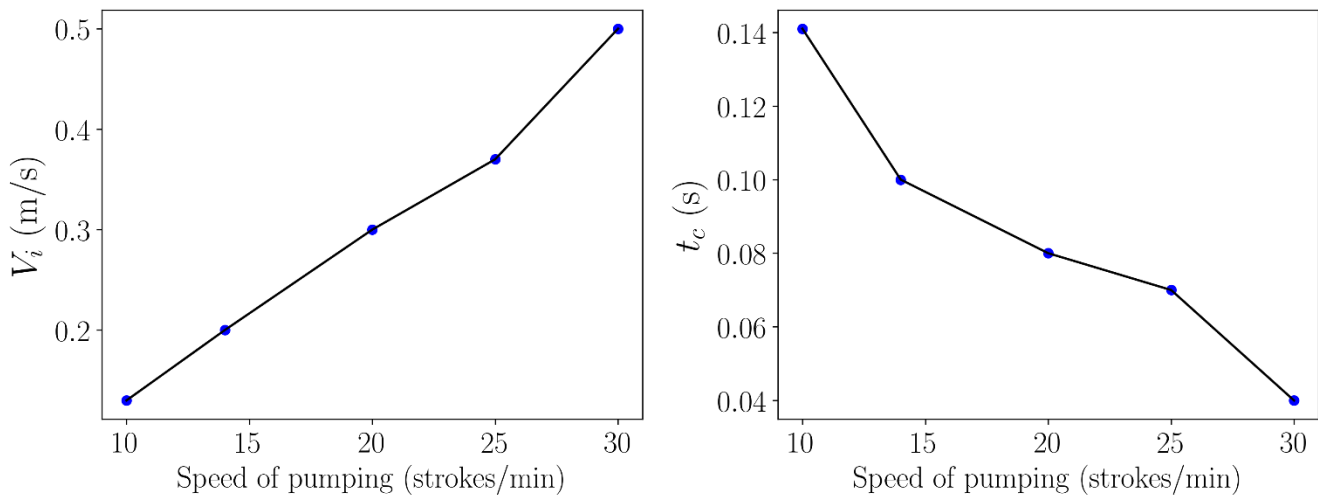


Figure 3 Typical variation in the speed of the ball during the valve closing process. The markers indicate the times at which the simulation results were collected.

We study the dependence of the speed of approach of the ball towards the seat during the valve closing process. The influence of two parameters; density of the ball material and the plunger speed, on the approach speed is examined by conducting a parametric study. A typical variation of the speed of the ball during the closing process is shown in Figure 3. The sharp dip in the graph indicates the initial acceleration of the ball in the negative direction, towards the seat, and then a deceleration back to zero speed in a short time, indicating the impact of the ball on the seat. From this data, we can measure the speed of the ball just before impact (V_i) and the time taken for the valve to close (t_c).



(a) Impact speed

(b) Closing time of SV

Figure 4 Linear variation of the impact speed of the ball on the seat (V_i) and the valve closing time (t_c) on the speed of pumping, or in other words the plunger speed (V_p).

In Figure 4, the impact speed (V_i) and the valve closing time (t_c) for five different plunger stroke times are shown. These plots show a clear linearly increasing trend of the impact speed with the stroke period, and a decreasing trend of the valve closing times with stroke period. This implies that higher plunger speeds, which is desirable in view of larger pump efficiency, lead to higher impact speeds, putting the pump under higher risk of damage. An optimum plunger speed should be chosen to avoid too high an impact speed and too low a pump efficiency. However, pump efficiency is not the only reason for choosing higher plunger speeds because, as will be discussed in the next section, too low a plunger speed can also result in a partially open valve, which is also not desirable.

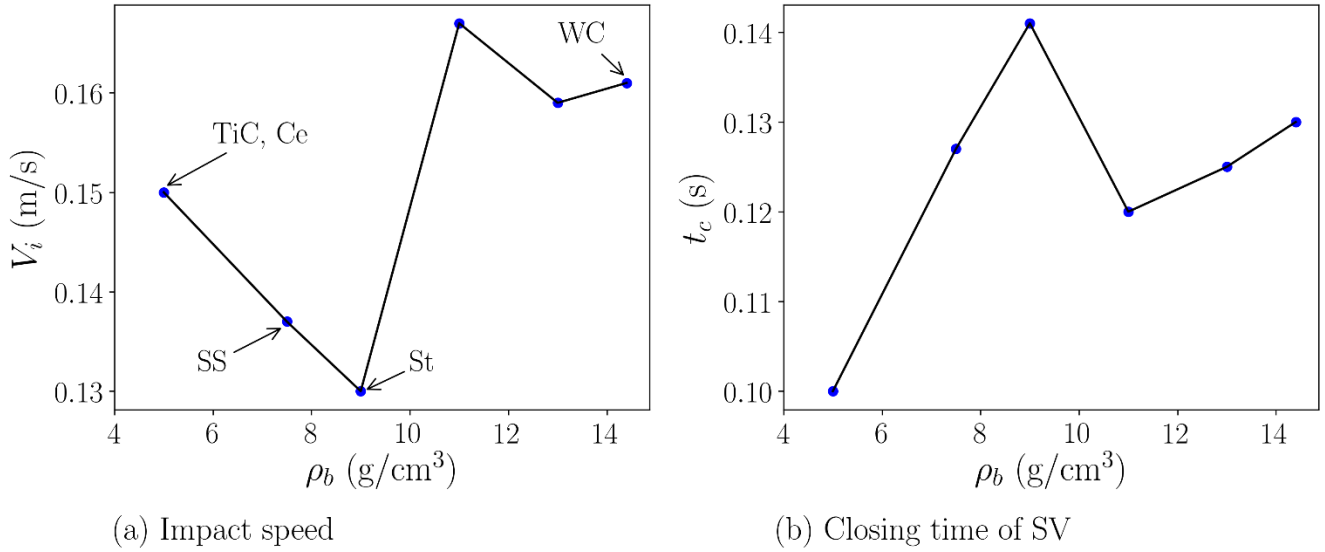


Figure 5 Variation of the impact speed of the ball on the seat (V_i) and the valve closing time (t_c) on the density of the ball material (the weight of the ball) for a pumping rate of 10 strokes per minute. The annotations in (a) indicate the usually used materials for the ball with the corresponding density values. WC: tungsten carbide, St: stellite, SS: stainless steel, TiC-WC: titanium carbide/tungsten carbide, Ce: ceramic. The solid lines are drawn only for clarity in presentation.

In Figure 5, the influence of the density of the ball material (ρ_b) on the two parameters is shown. Although the density of the ball changes by as much as three times from the lowest value to the highest, the variation of the impact speed is within 10% of its mean value. This indicates that the effect of the ball density or the ball weight for a given size of the ball does not have a significant influence on the impact speed or the valve closing times. The various contributions (weight, buoyancy, mass-specific viscous and pressure forces) to the acceleration of the ball is shown in equation 1.

$$a_b = \underbrace{g \left(1 - \frac{\rho_f}{\rho_b} \right)}_{\text{gravity + buoyancy}} + \underbrace{\frac{f_f}{m_b}}_{\text{viscous + pressure}} \quad (1)$$

The ball density affects the fluid motion and thus its acceleration via the ratio $\frac{\rho_f}{\rho_b}$, which varies only between ≈ 0.28 and 0.07 for the quite extensive variation of the density of the ball

considered in this study (see Figure 5). The contribution from the viscous and the fluid pressure to the motion of the ball is considered in the next section.

Valve opening

Although the ball density does not significantly influence the closing process, one clearly expects it to influence the opening process because the weight of the ball, which is dependent on the density of the ball material, should be balanced by the fluid dynamic forces for the valve to open. If the ball density is too high, then for a given size of the ball and plunger speed, the resulting fluid dynamic force may not be enough to lift the ball off the seat to open the valve. We consider the valve completely open when the ball hits the ceiling of the valve cage and remains there due to the balance between the weight, hydrodynamic force and the repulsive force pushing the ball away from the ceiling. This repulsive force is similar to the one applied between the ball and the seat to prevent solid-solid contact, and is activated only when the ball surface is within a small cut-off distance from the ceiling. However, in some cases, the hydrodynamic force may not be enough to push the ball all the way up to the ceiling, resulting in a partially open valve. Partially open valves are known to cause ball chatter and several other unwanted effects in the pump (Cutler & Mansure, 1999). One way to overcome this limitation is to increase the plunger speed to induce larger fluid dynamic force (through suction action), however, as seen in the previous section, higher plunger speeds result in proportionally larger impact speeds that might cause seat damage. In view of this, the aim is to find optimum values of the ball material density and the plunger speed.

The first step in this optimization procedure is to find those combinations of ρ_b and V_p that demarcate the boundary between fully open and partially open states of the valve. These critical values are dependent on the specific geometry of the valves, and hence we have to run fully resolved fluid flow simulations for a particular valve design. We demonstrate this procedure for the valve geometry shown in Figure 2 (b). In these simulations, only the SV is considered, and the TV is removed from the computational model to reduce computational complexity. However, the effect of the TV in its closed state is mimicked by applying a constant volume flux $Q = \pi(r_b + s)^2 V_p$ at the outlet of the SV. We have used this simplification because while studying the valve opening, we are interested only in the phase of the cycle when the TV is traveling upward. We start each run with the SV in closed position and allow for sufficient time so that the ball finally settles at a fixed position in the chamber: either within the fluid, in equilibrium with the fluid forces (partially open SV), or it even reaches the ceiling (fully open SV). In the first situation, the hydrodynamic pressure force only balances its weight. A two-dimensional matrix consisting of all combinations of values of ρ_b and V_p within their practically relevant ranges and parametrizing the runs is drawn up, and the simulations are carried out for all these values. From these results, we extract those pairs describing a ball just short of reaching the ceiling, i.e., approaching the ceiling but not touching it so that the repulsive force is not invoked. These operation conditions, separating those referring to a partially closed from those referring to a fully closed SV, are plotted as solid circles in Figure 6. Finding these relatively few (here three) critical combinations out of all (16 in our preliminary study) systematically represents a subtle numerical issue, which still opens room for improvement. Since the ratio of the ball/fluid densities is quite large, only points for which $\rho_b > 1$ have relevance. The origin is added though to guide the fitting process. Interestingly, the fitting process discloses a square-root variation (solid) of the critical plunger speed V_p over the critical ball density ρ_b . Operating the pump in the region below the square-root curve should be avoided in order to prevent partially opened valves, whereas operating conditions too remote from and above the curve is also not recommended in view of the imminent danger of seat damage due to correspondingly high ball impact speeds.

As a central finding, this curve can be used by pump designers and operators for ensuring that the pump is being used in an optimized condition.

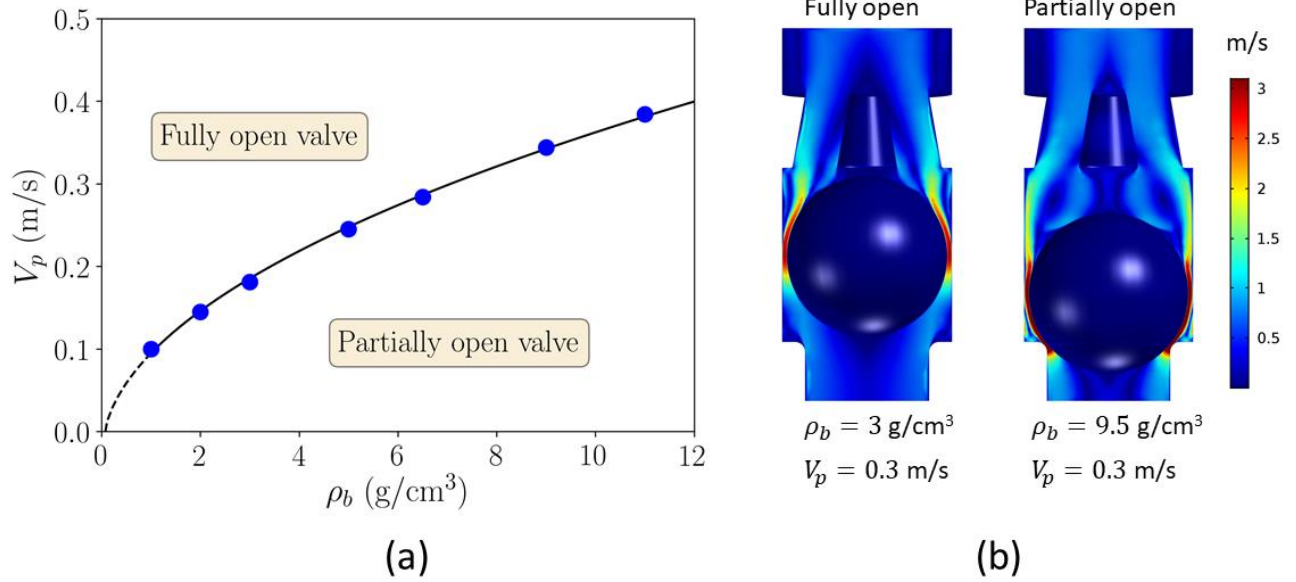


Figure 6 (a) Boundary between fully and partially open valve states. The valve is only partially open in the region below the square-root fit to the data in solid line. Further away the plunger speed is from the curve on the outside, larger is the impact speed of the ball on the seat. The dashed line is the extrapolation of the fitted curve. (b) Total velocity field shown for a fully and partially open valve. Sufficient time was allowed for the transients to die down before these data were collected.

Asking why the critical plunger speed (V_c) varies (approximately) with the square-root of the critical density (ρ_b) is, without doubt, a pivotal question. A preliminary (albeit not conclusive) answer is provided as follows. At first, this observation is advantageously cast into a non-dimensional number, called Optimum Valve (OMV) number and is defined by

$$N_{omv} = \frac{8}{3} \frac{g r_b}{\rho_f} \left(\frac{\rho_b}{V_p^2} \right) = \left(\frac{4\pi r_b^3 \rho_b g / 3}{\rho_f V_p^2 \pi r_b^2 / 2} \right) \quad (2)$$

The OMV number expresses the ratio of the two competing forces acting on the ball at the high Reynolds numbers at play (cf. Jalikop *et al.*, 2019): the weight of the ball ($\propto \rho_b$) over the dynamic pressure, where $\rho_b \propto V_p^2$ serves as the appropriate reference value. This number essentially captures the effect of valve geometry on its operation. Hence, for a particular valve, the OMV number can be extracted using our computational model by following the procedure described above. By definition, the OMV number expresses the ratio of the two competing forces acting on the ball at the high occurring Reynolds numbers (cf. Jalikop *et al.*, 2019): the weight of the ball involving its density over the dynamic pressure scaling with the square of the plunger speed. Most importantly, by dimensional arguments, and under the neglect of viscous forces acting on the ball, we expect the value of N_{omv} extracted from the simulated data being merely dependent on the pump geometry and only weakly on the kinematics of the plunger and the fluid properties: as inferred from the small density ratio in equation (1), the ball is essentially freely falling due to its weight during most of the cycle period. We therefore expect rather large values of N_{omv} , which only vary with V_p . Indeed, the square-root fit in Figure 6 gives $N_{omv} \approx 40$ for the valve geometry

we have considered in our simulations, which confirms the predominance of the gravitational acceleration in equation (1) over the fluid force density (f_f/m_b).

Given the small gap between the freely moving ball and wall of the cage (s), one can apply a basic inspection analysis to estimate the relative magnitudes of the fluid forces involved. To this end, we consider the contribution from a purely shear flow (called the Couette flow) to the fluid velocity to estimate the shear stress exerted on the plunger and the ball. The result of such an analysis shows that the viscous contribution to the hydrodynamic net force acting on the ball, expressed as (f_f) in equation 1, is negligibly small as long as $\sqrt{r_b/s} \ll Re_p$. Here $Re_p = V_p r_b / \nu$ is the suitably formed Reynolds number, based on the maximum plunger speed. In our case, the inequality is indeed satisfied as $\sqrt{r_b/s} (\approx 4) \ll Re_p (\approx 2 \times 10^4)$.

Hence, using our model, the OMV number for a given valve geometry can be computed and the operating conditions accordingly designed to achieve an optimized pump operation. In a nutshell, the OMV number gives the pump designer or the pump operator a rule of thumb in optimizing the pumping.

Mid-cycle valve closure

In the previous section we showed how our model can be used to understand valve opening/closing to optimize the valve design and pump operation through a valve optimization parameter, N_{omv} . In this section, we use a pump card from a real pump provided to us by an oil field operator and test if this parameter helps us understand the operation of a real pump. The advantage of using a coupled model is that one can simulate realistic conditions of down-hole pump operation by considering the exact opening and closing of valves and their influence on the pressure drop in non-ideal scenarios, for example, when there are fluctuations of plunger speed.

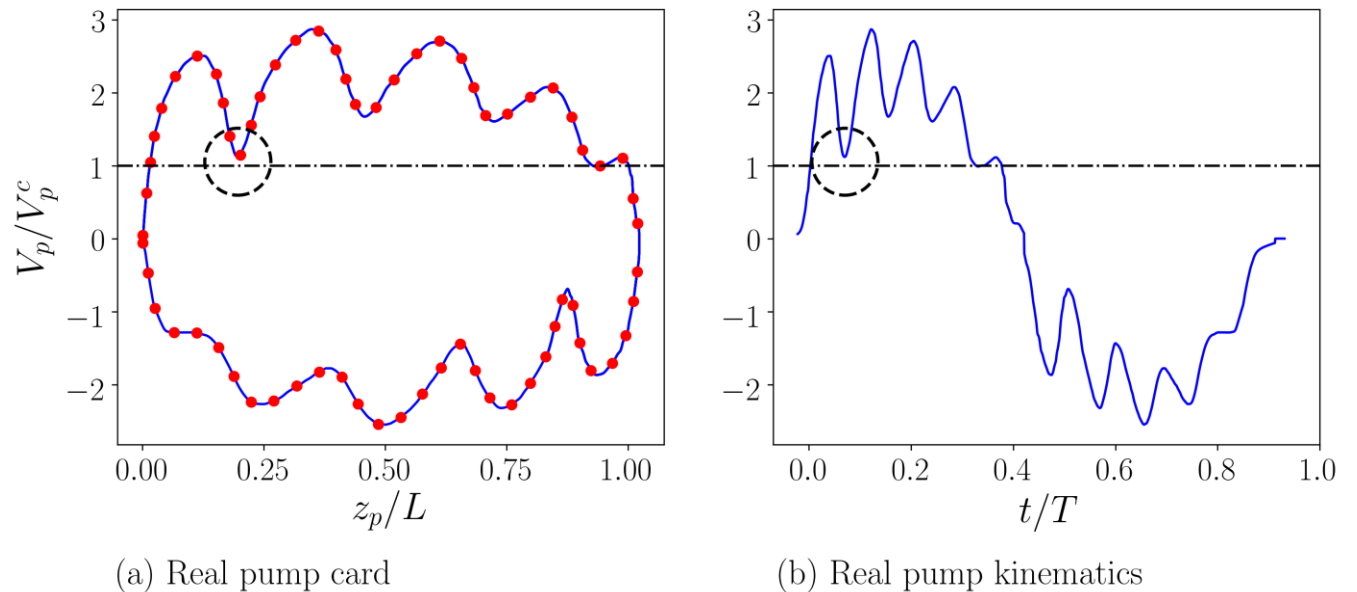


Figure 7 Speed of the plunger non-dimensionalized using the critical plunger speed as a function of (a) the non-dimensional position of the plunger for real pump card data, and (b) as a function of non-dimensionalized. Note in (a), the blue solid line is the fitted line to the data using spline interpolation of the pump card data shown in red dots. The dashed circles indicate the region where the plunger speed drops close to the critical plunger speed.

Here we consider the same pump for which we computed $N_{omv} \approx 40$ in the previous section, but use a real pump card as an input for the simulations. Unlike an ideal pump card, a typical real

pump card has fluctuations in the plunger speed, mainly due to the elasticity of the sucker rod (Gibbs, 1963). This pump card is shown in Figure 7, in which the plunger speed is non-dimensionalized by the critical speed obtained using the definition of the OMV number, $V_p^c = \sqrt{\frac{8g\rho_b}{3\rho_f N_{omv}}}$. The length and the time are non-dimensionalized by the pumping stroke length (L) and the pumping time period (T), respectively. We simulate two entire pump cycles, $L = 2.5$ m, and observe the effect of fluctuations of the speed of the TV on the open state of the SV. In particular, we are interested in studying the interaction between the coupled valves in the region close to the first dip in speed during the up-stroke, where the plunger speed drops close to the critical speed ($\frac{V_p}{V_p^c} = 1$). The results presented here are from the second pump cycle, during which all the transients have already died down and the motion of the balls has reached a steady cycle.

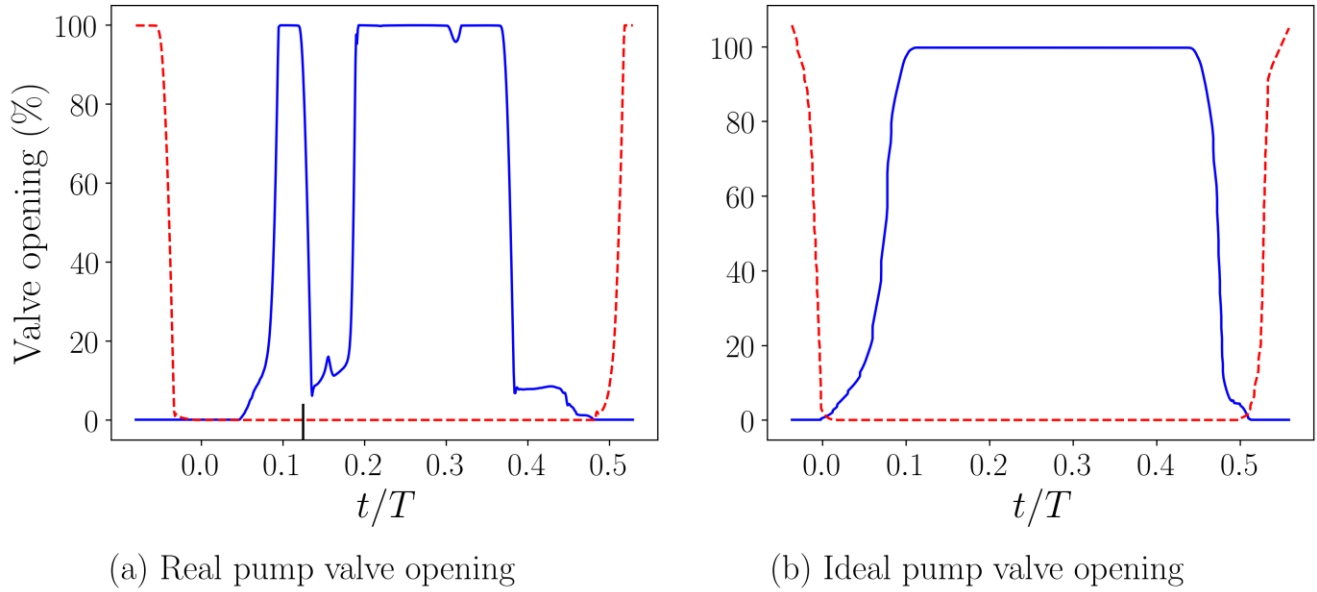


Figure 8 Degree of valve opening of SV (in blue solid line) and TV (in red dashed line) for (a) real pump card data and (b) ideal cases without plunger speed fluctuations. Note the closing of SV in mid-cycle where, ideally, SV is fully open and TV is fully closed.

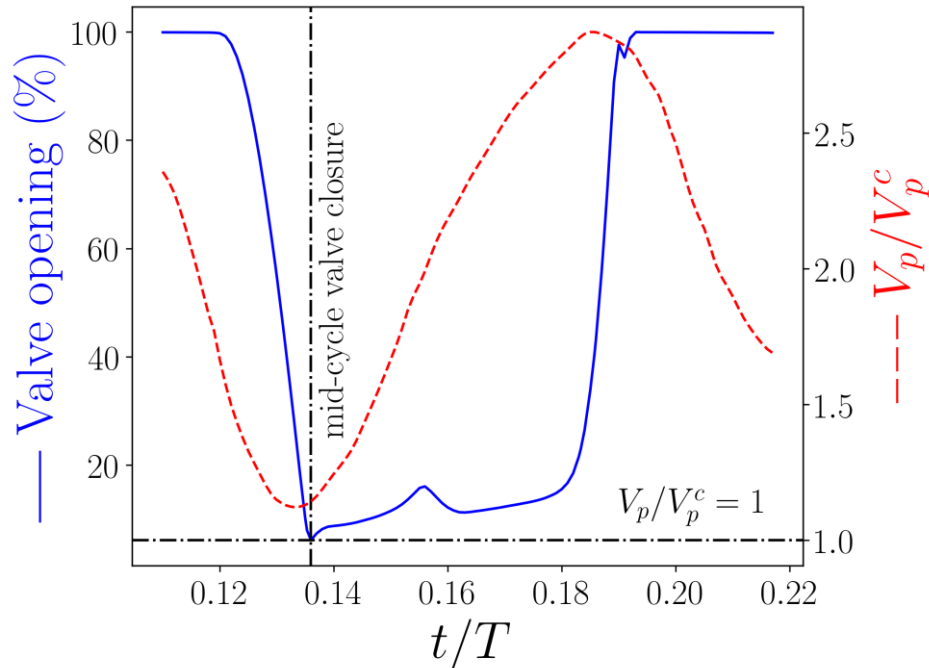


Figure 9 Close-up of the region where the mid-cycle valve closure occurs, which coincides with the drop in plunger speed to a value close to the critical plunger speed estimated for the value of N_{omv} in our simulations.

The degree of valve opening can be plotted as a ratio of the distance between the ball surface from the seat and the total length of ball motion along the cage (l , see Figure 2). In Figure 8, the valve opening of SV for the real and ideal cases are plotted. It can be observed that in the real case, the SV closes in mid-cycle, where ideally it should be open as seen in Figure 8 (b). A closer look at this region in Figure 9 shows that less than 10 % of the valve is open, and it coincides with the dip in the plunger speed as seen in the pump card (Figure 7) closer to where $\frac{V_p}{V_p^c} = 1$. Hence, when the speed of the TV momentarily drops close to the critical speed estimated from the OMV number, the drag force on the on the SV ball becomes smaller than its weight and the ball drops back to the seat of the SV, resulting in mid-cycle valve closure. This scenario can pose a serious danger to the pump because the relatively high speed of the plunger (compared to the speed during ideal valve closing process) accompanied by a narrow constriction between the ball and the seat causes an undesirably large pressure drop across the valve and especially in the constriction itself. Moreover, the rise in plunger speed immediately after its drop intensifies the adverse effect of mid-cycle valve closure. This is because, as the ball accelerates towards the seat, the increasing region of the plunger fluctuation kicks in and draws the fluid faster into the chamber. However, because of the ball's inertia, there is a finite time before the ball slows down to zero velocity and turns around to start climbing up back to the ceiling during which the ball has dropped further down. This, however, narrows the gap during the same time the increasing plunger speed is increasing the fluid velocity in the gap. This critical combination of increased fluid speed and decreasing gap results in a higher pressure drop in the gap (p_{gap}^{SV}) during the mid-cycle valve closure compared with the normal closing process, as seen in Figure 10.

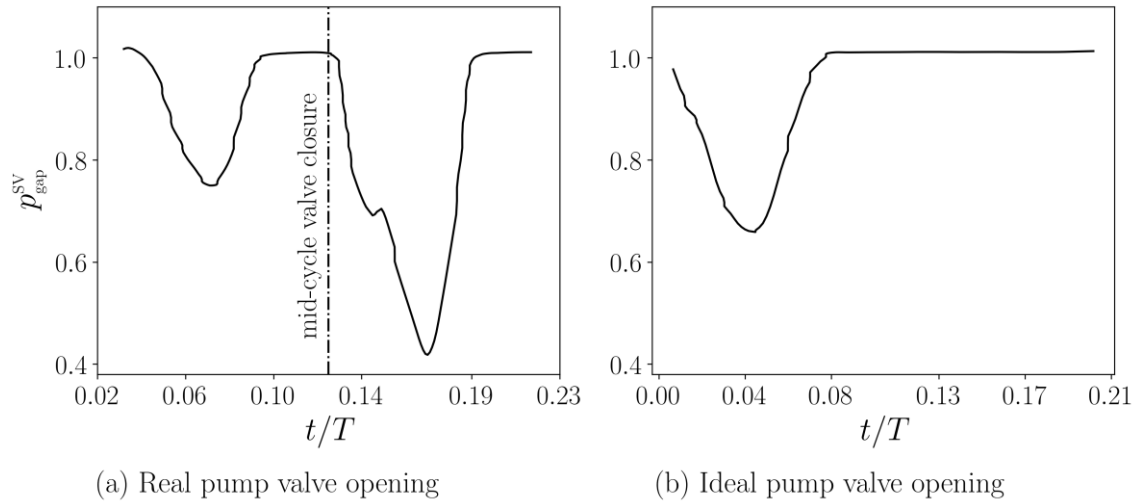


Figure 10 Pressure in the gap between the ball and the seat of the SV during mid-cycle valve closure in the real pump card data (a). The corresponding region for the ideal case is shown in (b), where the second pressure drop seen in (a) is absent. The first pressure drop seen in both the cases is from the valve opening process.

Pressure drops, such as the one illustrated above, can release dissolved gases that may potentially lead to phenomena such as fluid pound and gas interference, which are common causes of pump damage encountered in the petroleum industry. Hence, mid-cycle valve closure could in principle be an underlying cause of these non-ideal scenarios associated with real pump cards. If this is verified by experimental or direct measurements in down-hole pumps, our model could be used to compute the OMV number for a given pump geometry and hence be used in pump design and operation.

Once, the N_{omv} is computed for a given pump geometry, the pump operator can use it to maintain the speed of the plunger above the danger zone, i.e. $V_p > V_c(N_{omv})$. During the pump design phase, on the other hand, the OMV number can be used to choose the right material for the ball so that pump can be operated safely without compromising on its efficiency.

Conclusions

In this work, we have applied a previously introduced fluid dynamics model for down-hole pumps to calculate parameters that will aid pump designers and oil field operators with maximizing the service life and safety of their ball valves. In particular, we produced a map that shows which combinations of ball density and pumping speed lead to fully open or only partially open valves for a given valve cage geometry. The boundary between these two operational states can be parametrized using the newly introduced optimum valve number N_{omv} , a scalar that depends only on the cage geometry. The knowledge of this parameter can be used as novel design rule for the optimization of the operational state of a pump. Refining the numerical strategy to compute N_{omv} efficiently is an indicated topic of future efforts.

The second application of our model is the identification and the discussion of the ramifications of mid-cycle valve closure. This phenomenon that has yet to be experimentally observed, may be an important reason for premature valve failures, as it can multiply the number

of ball–valve impacts during operation and lead to steep pressure gradients near the valve seat that may cause seat damage associated with the collapse of microscopic gas bubbles. With our model, it will be possible to estimate the probability of such a mid-cycle valve closure for a given pump geometry and pump card, allowing the designer or operator to counter the effect, e.g., by selecting a lighter ball or by increasing the pumping speed.

Thus, by providing a tool to avoid pump designs or operational states that are prone to incipient seat damage by impact or fluid-dynamics-related causes, it is possible to delay secondary damage such as erosion, which ultimately leads to costly valve replacement.

Acknowledgments

We would like to thank the Austrian COMET Program (project K2 XTribology, no. 849109 and project K2 InTribology, no. 872176) for funding, and the work was carried out at the “Excellence Centre of Tribology” AC2T research GmbH.

Nomenclature

f_f	Fluid force, N
g	Acceleration due to gravity, m/s ²
l	Maximum displacement of the ball inside the cage, m
L	Stroke length of the pump, m
m_b	Mass of the ball, kg
$N_{omv} = \frac{8g}{3\rho_f} \left(\frac{V_b}{V_p^2} \right)$	OptimuM Valve (OMV) number
ν	Kinematic viscosity of the fluid, m ² /s
PIP	Pump Intake Pressure, Pa
p_{gap}^{SV}	Pressure at the center of the gap between the ball and the seat, Pa
Q	Volume flow rate, m ³ /s
r_b	Radius of the ball, m
ρ_b	Density of the ball material, kg/m ³
ρ_f	Density of the fluid, kg/m ³
$Re_p = \frac{r_b V_p}{\nu}$	Reynolds number
s	Clearance gap between the ball and the cage wall, m
SV	Standing Valve
TV	Traveling Valve
t	Time, s
t_c	Time taken by the valve closing process, s
T	Time period of the pump cycle, s
TP	Tubing Pressure, Pa
V_b	Speed of the ball, m/s
V_i	Impact speed of the ball on the seat, m/s
V_p	Speed of the plunger, m/s
$V_p^c = \sqrt{\frac{8g\rho_b}{3\rho_f N_{omv}}}$	Critical speed of the plunger, m/s

References

- Cutler, R.P., Mansure, A.J., 1999. Fluid Dynamics in Sucker Rod Pumps. *Sandia National Laboratories Technical Report*.
- Davis, R.H., Serayssol, J.-M., Hinch, E.J., 1986. The elastohydrodynamic collision of two spheres. *J. Fluid Mech.* **163**, 479–497.
- Domnick, C.B., Benra, F.-K., Brillert, D., Dohmen, H.J., Musch, C., 2017. Investigation on flow-induced vibrations of a steam turbine inlet valve considering fluid–structure interaction effects. *J. Eng. Gas Turbines Power* **139** (2), 022507.
- Domnick, C.B., Brillert, D., 2019. Flow-induced steam valve vibrations—A literature review of excitation mechanisms, preventive measures, and design improvements. *J. Eng. Gas Turbines Power* **141** (5), 051009.
- Doty, D.R., Schmidt, Z., 1983. An improved model for sucker rod pumping. *Soc. Pet. Eng. J.* **23** (1), 33–41.
- Gibbs, S.G., 1963. Predicting the behavior of sucker-rod pumping systems. *J. Pet. Technol.* 769–778.
- Hoy, M., Kometer, B., Bürßner, P., Puscalau, G., Eder, S., 2018. SRP equipment customization creating value by increasing run life in a low oil price environment. In: SPE Artificial Lift Conference and Exhibition. SPE-190958-MS.
- Iannetti, A., Stickland, M.T., Dempster, W.M., 2014. A computational fluid dynamics model to evaluate the inlet stroke performance of a positive displacement reciprocating plunger pump. *Proc. Inst. Mech. Eng. A* **228** (5), 574–584.
- Jalikipo S., Scheichl B., Hönig S., 2019 Eder S.J.: Simulation-aided identification of mid-cycle valve closure in a down-hole pump, *J. of Fluids and Structures*, **91**, 102774, Elsevier B.V., 102774
- Katsich, C., Cihak-Bayr, U., Hönig, S., Eder, S.J., 2019. From test rig to down-hole pump: Ranking material pairings for ball valves according to their impact wear resistance. *Tribol. + Schmier.* **66**, 14.
- Lekia, S.D.L., Evans, R.D., 1995. A coupled rod and fluid dynamic model for predicting the behavior of sucker-rod pumping systems-part 1: Model theory and solution methodology. *SPE Prod. Facil.* **10** (1), 26–33.
- Li, W., Dong, S., and Sun, X., 2018. An Improved Sucker Rod Pumping System Model and Swabbing Parameters Optimized Design. *Math. Problems in Engg.*, **2018**, Article ID 4746210
- Lyons, W.C., Plisga, G.J., Lorenz, M.D., 2016. Standard Handbook of Petroleum and Natural Gas Engineering. Gulf Professional Publishing, Elsevier, 6-152.
- Romero, O.J., Almeida, P., 2014. Numerical simulation of the sucker-rod pumping system. *Ing. Investig.* **34** (3), 4-11.
- Samad, A., 2010. Gas interference in sucker rod pump. In: International Conference on Modeling, Optimization and Computing (ICMOS 2010), **1298**. American Institute of Physics, 274-281.
- Scheichl, B., Neacșu, I.A., Kluwick, A., 2015. A novel view on lubricant flow undergoing cavitation in sintered journal bearings. *Tribol. Int.* **88**, 189–208.
- Weaver, D.S., Ziada, S., Au-Yang, M.K., Chen, S.S., Païdoussis, M.P., Pettigrew, M.J., 2000. Flow-induced vibrations in power and process plant components — progress and prospects. *J. Press. Vessel Technol.* **122**, 339–348.